

# Flame-Acoustics Interaction of Flames Propagating in a Narrow Duct: Effect of Heat Losses and Lewis Number

Carmen Jiménez, Vadim N. Kurdyumov,  
CIEMAT  
Madrid, Spain

## 1 Introduction

In a recent work [1] we showed that for narrow adiabatic channels, flames with  $Le = 1$  propagating from an open to a closed end can be symmetric with a tulip shape or non-symmetric. This symmetry breaking, independent of the acoustics, was previously studied in a series of works [2–9], where it was shown to be linked to hydrodynamic and thermodiffusive instabilities. so that non-symmetric flames can appear for a certain range of values of parameters such as the channel width, wall thermal properties, gas thermal expansion coefficient, reactants flow rate and Lewis number. The two type of solutions, symmetric and non-symmetric, can simultaneously appear, with non-symmetric flames being usually stable while symmetric flames are unstable, and they present very different burning speeds (non-symmetric flames are much faster). The coupling flame-acoustics was shown in [1] to depend on the flame shape, so that symmetric and non-symmetric flames not only propagate at different speeds but also present different oscillating behaviour. Here we study the effect of the wall thermal properties and differential diffusion in the flame shape and its oscillating behaviour under acoustic coupling.

## 2 Mathematical Formulation and Numerical Treatment

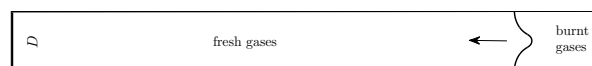


Figure 1: Sketch of the problem

We consider a premixed flame propagating in an open-closed 2D channel of width  $D$  and length  $L$ , filled with a fuel/air mixture at initial temperature  $T_0$ . A flame front propagating from the open to the closed end (right to left in Fig. 1) can be symmetric or non-symmetric [1–7, 9]. The exact shape and burning rate of this flame can be determined numerically by solving the governing equations of the problem. We neglect body forces, radiation heat losses and heating by viscous dissipation, and assume a one-step irreversible chemical reaction  $F + O \rightarrow P$ , deficient in fuel, so that the reaction rate is  $\dot{\omega}_F = \mathcal{B} \rho^2 Y_F \exp(-E_a/\mathcal{R}T)$ , with  $E_a$  the activation energy and  $\mathcal{B}$  the pre-exponential factor. The

resulting conservation equations for mass, momentum, energy and fuel mass fraction are:

$$\frac{\partial \rho}{\partial t} + \frac{\partial \rho u_i}{\partial x_i} = 0 \quad (1)$$

$$\frac{\partial \rho u_i}{\partial t} + \frac{\partial \rho u_i u_j}{\partial x_j} = -\frac{\partial p}{\partial x_i} + \frac{\partial \tau_{ij}}{\partial x_j} \quad (2)$$

$$\frac{\partial \rho e_t}{\partial t} + \frac{\partial (\rho e_t + p) u_i}{\partial x_i} = \frac{\partial u_i \tau_{ij}}{\partial x_j} - \frac{\partial q_i}{\partial x_i} + Q \dot{\omega}_F \quad (3)$$

$$\frac{\partial \rho Y_F}{\partial t} + \frac{\partial \rho Y_F u_i}{\partial x_i} = \frac{\partial}{\partial x_j} \left( \rho \mathcal{D} \frac{\partial Y_F}{\partial x_j} \right) - \dot{\omega}_F, \quad (4)$$

with  $u_i$  the components of the gas velocity,  $\rho$  its density,  $p$  the pressure,  $Y_F$  the fuel mass fraction and  $e_t$  the total (non-chemical) energy, defined as  $e_t = \frac{1}{2} u_k u_k + p/\rho (\gamma - 1)$ , with  $\gamma = c_p/c_v$ , the relation of heat capacities, assumed constant, and where the perfect gases equation of state:  $p = \rho \mathcal{R} T = \rho (c_p - c_v) T$  is used. These equations are completed by the definition of the viscous stress tensor,  $\tau_{ij} = \mu (\partial u_i / \partial x_j + \partial u_j / \partial x_i - \frac{2}{3} \delta_{ij} \partial u_k / \partial x_k)$ , and the heat flux vector,  $q_i = -\lambda \partial T / \partial x_i$ , where  $\lambda = \mu c_p / Pr$  is the gas thermal conductivity of the gas, defined as a function of the mixture viscosity  $\mu$ , its heat capacity  $c_p$  and a constant Prandtl number  $Pr$ . The viscosity and conductivity are assumed here to vary with temperature, as  $\mu/\mu_0 = \lambda/\lambda_0 = (T/T_0)^{0.7}$ , while the fuel diffusivity  $\mathcal{D}$  is  $\mathcal{D} = \mathcal{D}_T / Le = \lambda / (\rho c_p Le)$ , with  $Le$  a constant Lewis number, and depends on temperature as  $\rho \mathcal{D} / \rho_0 \mathcal{D}_0 = (T/T_0)^{0.7}$ . The subscript 0 stands for quantities evaluated in the fresh gas mixture.

We introduce the Zel'dovich number  $\beta = E_a (T_a - T_0) / (\mathcal{R} T_a^2)$  and the thermal expansion parameter  $q = T_a / T_0$ , the standard parameters characterizing Arrhenius models, with  $T_a$  the adiabatic flame temperature. The heat produced per unit volume and time,  $Q \dot{\omega}_F$ , is given by the factor  $Q = (T_a - T_0) c_p / Y_{F0} = (q - 1) T_0 c_p / Y_{F0}$ , where  $Y_{F0}$  represents the fuel mass fraction in the fresh gas mixture.

We solve a dimensionless version of Eqs. 1-4, scaled with the thermal flame thickness of the planar flame, defined as  $\delta_T = \mathcal{D}_{T0} / S_L$  (with  $\mathcal{D}_{T0}$  the thermal diffusivity of the fresh gas mixture,  $\mathcal{D}_{T0} = \lambda_0 / (\rho_0 c_{p0})$ , and  $S_L$  the laminar planar flame speed), a time scale  $\delta_T / c_0$  (with  $c_0$  the speed of sound in the fresh gases,  $c_0 = \sqrt{\gamma p_0 / \rho_0}$ ), and the fresh gases reference state given by  $\rho_0, T_0, \mu_0, Y_{F0}$  and  $c_{p0}$ . For these dimensionless equations the only free parameters are  $Le, Pr, q, \beta, \gamma$ , a Damköhler number  $Da$  related to the pre-exponential factor  $\mathcal{B}$  as  $Da = \mathcal{B} \rho_0 \delta_T / c_0$ , and an acoustic Reynolds number  $Re_{ac} = \delta_T c_0 / \nu_0$ , which relates  $\delta_T, c_0$  and the fresh gases kinematic viscosity  $\nu_0 = \mu_0 / \rho_0$ . In the present work we choose a set of fixed parameters  $Pr = 0.7, \gamma = 1.4, q = 8, \beta = 10, Re_{ac} = 476.19$  and vary the Lewis number  $Le$  and the wall thermal properties, as explained later. The Damköhler number  $Da$  was chosen to vary with  $Le$ , so that for all the flames presented below the planar flame speed  $S_L$  takes the value  $S_L = 3 \times 10^{-3} c_0$ .

The computational domain, a  $D \times L$  rectangle, is discretized on a uniform Cartesian grid with  $100 \times 2000$  cells for a channel with  $D = 40 \delta_T$  and  $L = 800 \delta_T$ . Grid refinement studies were conducted for selected cases, showing no appreciable differences in the results of simulations when the grid resolution was doubled or even quadrupled (see [1]). Note that for some particular cases a grid with finer resolution was required; this will be discussed in the text as these cases are presented. The time step is determined by a CFL condition based on the sound speed with a value 0.5 for the CFL factor.

Boundary conditions at the walls represent the solid-gas interaction. If the wall thickness  $h_w$  is assumed to be small,  $h_w / D \ll 1$ , then the temperature distribution within the solid wall can be taken as linear between the gas temperature and the external wall temperature, which we assume to be  $T_0$ , and we can write the temperature boundary conditions for the bottom and top walls as done in [3] or [7]:

$$\frac{\partial T}{\partial y} \Big|_{y=0} = \frac{\lambda_w}{\lambda_g h_w} (T_{y=0} - T_0), \quad \frac{\partial T}{\partial y} \Big|_{y=D} = \frac{\lambda_w}{\lambda_g h_w} (T_0 - T_{y=D}), \quad (5)$$

where  $\lambda_g$  and  $\lambda_w$  are the gas and wall thermal conductivities. The boundary condition for the left wall is set as adiabatic. These conditions are supplemented by no-slip conditions for velocity and no-flux conditions for the species at the walls.

The parameter  $\frac{\lambda_w}{\lambda_g h_w}$  controls the heat transfer between the gas and the solid and depends on the wall thermal conductivity and thickness, which are constants, as well as on the gas thermal conductivity,  $\lambda_g$ , which varies with temperature. We will use, as in [7], a reference non-dimensional heat transfer parameter given by the value of the heat transfer parameter at the fresh gases scaled with the flame thickness  $\delta_T$ :

$$b = \frac{\lambda_w}{\lambda_g^0} \frac{\delta_T}{h_w}, \quad (6)$$

with  $\lambda_g^0$  the thermal conductivity of the unburned mixture. A value of the heat transfer parameter  $b = 0$  corresponds to an adiabatic wall and the limit  $b \rightarrow \infty$  represents isothermal walls.

At the open channel end a pressure node with constant pressure equal to ambient pressure ( $p = p_{atm}$ ) is set, representing an outlet open to the atmosphere, as in [1]. The NSCBC methodology [10] is used to implement the boundary conditions. Note that in some cases with very strong acoustic oscillations, the flow direction in the burnt gases may be occasionally inverted, so that the outlet becomes an inlet. In this case, additional conditions of zero gradient for the fuel mass fraction and temperature at the boundary are used.

We use, as in [1], the compressible solver NTMIX3D, a parallel solver designed for the direct numerical simulation of flames and turbulent reacting flows described in [11], using 6th-order finite differences and 3d-order Runge-Kutta time integration.

### 3 Results: symmetric and non-symmetric flame solution in a channel with heat losses

Two types of simulations are presented below: full domain simulations initialized from a planar flame with a non-symmetric perturbation (a hot spot in front of the flame at  $y = D/2$ ) and simulations using half the computational domain,  $0 < y < D/2$ , with symmetry imposed along the central axis  $y = D/2$ . As shown in [1], in the full domain simulations the flame becomes non-symmetric when this kind of solution is the stable solution while in the half domain simulations, the symmetry of the flame is forced.

Full domain simulations for  $Le = 1$  flames in a  $D = 40\delta_T$ ,  $L = 2400\delta_T$  channel show that for small heat losses the flame becomes rapidly non-symmetric while for large heat losses the flame remains symmetric. This can be seen in Fig. 2 left, where the flame is non-symmetric for the adiabatic ( $b = 0$ ) and moderate heat transfer ( $b = 0.01$ ) cases, becomes almost planar for  $b = 0.02$  and then symmetric with a mushroom shape for larger heat losses. This confirms that stabilization of symmetric flames is favored by heat losses as reported before in [7, 9]. While the non-symmetric flames obtained for  $b = 0$  or  $b = 0.01$  present large oscillations in the flame shape (and length and burning speed) along the full channel, these oscillations become much smaller for the case  $b = 0.02$ , with only appreciable oscillations at the end of the channel, where the flame has acquired a little curvature. Finally, for large values of the heat losses coefficient the flame adopts a symmetric mushroom shape and oscillations appear early in the channel propagation, but flames are extinguished by heat losses before these oscillations become important.

Half domain simulation results for the same parameters are presented in Fig. 2 right, showing a symmetric tulip shape for low heat losses ( $b = 0$ ), a planar flame for  $b = 0.01$ , a planar flame that becomes mushroom-shaped symmetric at the end of the channel for  $b = 0.02$ , and a mushroom symmetric flame for  $b = 1$ . The last two cases show flames identical to those obtained in the full domain. Oscillations in the flame shape are small in all cases. Note that in [1] it was shown that the flame response to acoustic

pressure oscillations, the flame transfer function, depends on the flame shape, and presents a different frequency dependence for symmetric and non-symmetric flames. For the present flame and channel size parameters, non-symmetric flames appear to present a more intense response to the eigen acoustic modes of the channel.

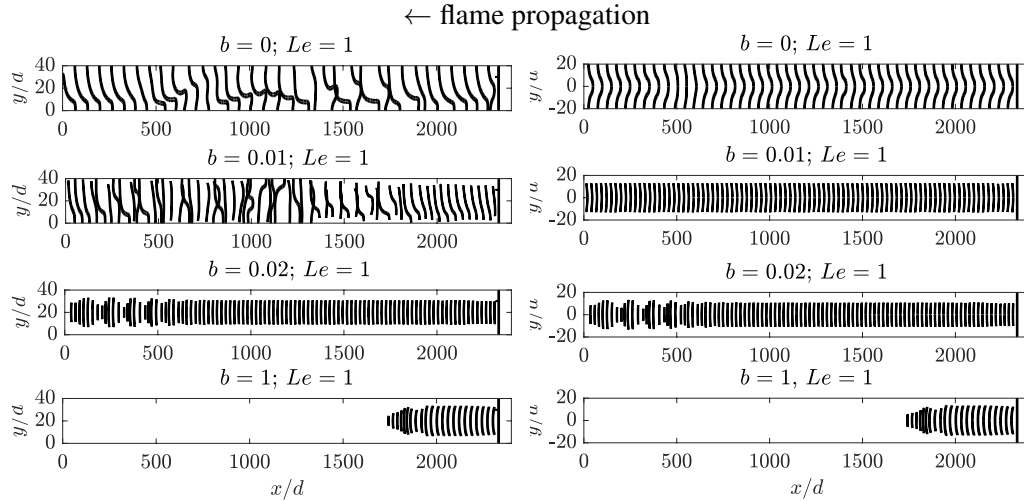


Figure 2: Flame propagation, represented by a heat release rate isoline at  $\omega = 1.5\rho_0c_0/\delta_T$ , plotted at time steps  $\Delta_t = 0.0125L/S_L$ , for  $Le = 1$  flames in a  $D = 40\delta_T$ ,  $L = 2400\delta_T$  channel with varying  $b$ , in full-domain (left) and half-domain (right) computations. The initial planar flame is near the right end.

#### 4 Effect of the Lewis number

Figure 3 presents the flame consumption speed  $S_c/S_L$ , the pressure at the end wall  $p_w/p_a$  and the flame shape for different Lewis number flames propagating in a channel with  $D = 40\delta_T$  and  $L = 800\delta_T$  and varying wall-thermal properties. We measure the flame burning rate, or consumption speed, (scaled with  $S_L$ ) by the integral:  $S_c/S_L = 1/\rho_0 Y_{F0} D S_L \int_0^D \int_0^L \omega_F dx dy$ . All the results in this section correspond to full-domain unsteady simulations initialized from a planar flame with a non-symmetric perturbation.

For  $Le = 1$  flames (left column), results are similar to those of the previous section: non-symmetric flames are found for low heat losses, the flame shape becomes planar as heat losses increase and then symmetric with mushroom shape for larger heat losses. However, contrary to what we observed in the longer channel of Fig. 2, for this channel with  $L = 800\delta_T$  oscillations are negligible for non-symmetric flames while they can become relatively important (up to 5% of  $p_a$ ) for symmetric flames. This is again a confirmation that the flame response at a given frequency is different for symmetric and non-symmetric flames. Because the longitudinal acoustic eigen frequencies in the channel depend on the channel length  $L$  (see [1]), the flame response changes when  $L$  is changed.

When the Lewis number is varied, the flame shape changes and, accordingly, the response to acoustic oscillations changes as well. For  $Le = 0.7$ , the flame in the adiabatic channel becomes non-symmetric, but with a different shape, more corrugated than in the  $Le = 1$  case. Because of this change in shape, the flame burning rate and the pressure oscillations are more important in this case than in the  $Le = 1$  case of the left column. As the heat losses coefficient is made larger, the flame shape becomes closer to planar and oscillations disappear. For  $b = 0.05$  we find symmetric flames oscillating between tulip and mushroom shape, with large oscillations in the flame consumption speed and in the pressure at the end wall, which can become as large as  $30S_L$  and  $50\%p_a$ , respectively. Finally, for values of the heat transfer coefficient  $b \geq 0.1$  the flame oscillations are damped, and the flame recovers a behaviour close

to that of the  $Le = 1$  flame, extinguishing before reaching the mid-channel. Apparently, these flames extinguish before reaching the position corresponding to the more resonant frequencies.

Finally, for  $Le = 0.3$  the flame shape changes drastically, and so do the propagation and oscillation characteristics. In the adiabatic and lower heat losses cases ( $b = 0, 0.01$  and  $0.02$ ), we observe symmetric flames which become non-symmetric along the propagation. Both the symmetric and the non-symmetric flames are very convoluted for this low value of  $Le$ , and as such, present a large surface and large burning rates, up to  $30 - 40$  times  $S_L$ . Oscillations in the flame speed and pressure are also very large, of the order of  $30S_L$  and  $50\%p_a$ , respectively. These fast flames reach very quickly the end wall. Finally, it is remarkable that large values of  $b$ , the flames adopt very high curvatures, even breaking into smaller round-shaped cells. This shape confers robustness to the flames, so that even for the largest heat losses these flames can propagate to the end of the channel. This kind of flames were observed before in [12] in simulations of flames in a Hele-Shaw chamber, also for low Lewis number and large heat losses. Here we report that these flames, in addition to a large propagation speed with large resistance to extinction by heat losses, might be linked to large pressure oscillations, as seen for  $b = 0.1$  and  $b = 1$  in Fig. 3.

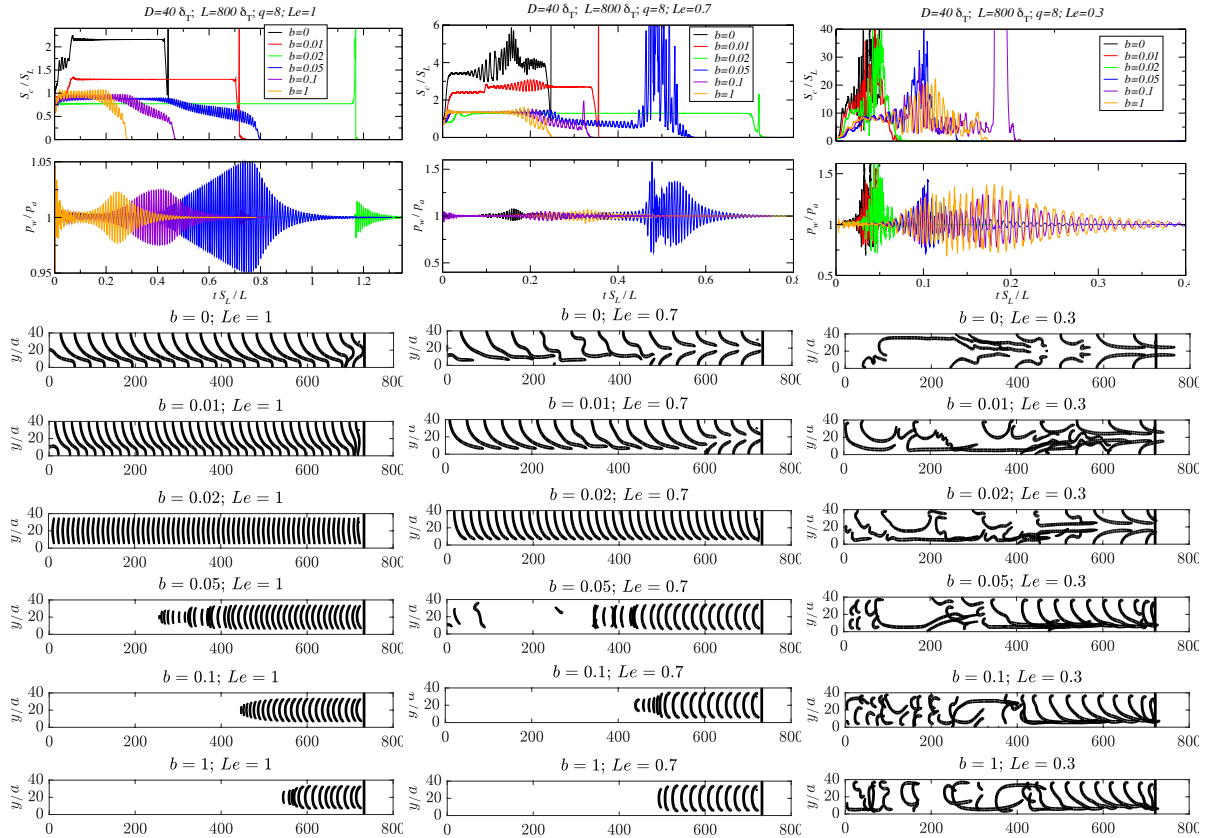


Figure 3: The flame propagation speed, the pressure at the end wall and the flame shape for  $Le = 1$ (left),  $0.7$ (middle) and  $0.3$ (right) flames in channels with  $D = 40\delta_T$ ,  $L = 800\delta_T$  and several  $b$  values. The flame profiles correspond to the isoline at  $\omega = 1\rho_0c_0/\delta_T$  plotted at times given by  $\Delta t = 0.01875L/S_L$  (cases  $Le = 1, 0.7$ ) and  $\Delta t = 0.0075L/S_L$  (case  $Le = 0.3$ ).

## 5 Summary and Discussion

We studied numerically the effect of the wall thermal properties and the Lewis number on the flame shape and, as a consequence, on the flame-acoustics interaction, for flames propagating in a narrow

open-closed channel. For  $Le = 0.7$  and  $1$ , flames are non-symmetric for low values of the heat transfer coefficient  $b$  and become mushroom-shaped symmetric for large values of  $b$ , extinguishing as  $b$  grows. The acoustic oscillations are important for non-symmetric flames in long channels and for symmetric flames in the case of shorter channels. For  $Le = 0.3$ , flames appear to be non-symmetric for all the studied values of  $b$ , breaking into small round-shaped cells as the heat transfer coefficient  $b$  becomes large. These cellular flames do not extinguish and propagate to the channel end. All the studied  $Le = 0.3$  flames present large pressure oscillations.

## References

- [1] C. Jiménez, D. Fernández-Galisteo, V. Kurdyumov (2021), Flame-acoustics interaction for symmetric and non-symmetric flames propagating in a narrow duct from an open to a closed end, *Combust. Flame* 225: 499.
- [2] V. N. Kurdyumov (2011), Lewis number effect on the propagation of premixed flames in narrow adiabatic channels: Symmetric and non-symmetric flames and their linear stability analysis, *Combust. Flame* 158: 1307.
- [3] V. Kurdyumov, C. Jiménez (2014), Propagation of symmetric and non-symmetric premixed flames in narrow channels: influence of conductive heat-losses, *Combust. Flame* 161: 927.
- [4] M. Sánchez-Sanz, D. Fernández-Galisteo, V. Kurdyumov (2014), Effect of the equivalence ratio, Damköhler number, Lewis number and heat release on the stability of laminar premixed flames in microchannels, *Combust. Flame* 161: 1282.
- [5] D. Fernández-Galisteo, C. Jiménez, M. Sánchez-Sanz, V. Kurdyumov (2014), The differential diffusion effect of the intermediate species on the stability of premixed flames propagating in microchannels, *Combust. Theory Model.* 18: 582.
- [6] C. Jiménez, D. Fernández-Galisteo, V. Kurdyumov (2015), DNS study of the propagation and flashback conditions of lean hydrogen-air flames in narrow channels: Symmetric and non-symmetric solutions, *Int. J. Hydrogen Energy* 40: 12541.
- [7] C. Jiménez, V. Kurdyumov (2017), Propagation of symmetric and non-symmetric lean hydrogen-air flames in narrow channels: Influence of heat losses, *Proc. Combust. Inst.* 36: 1559.
- [8] A. Dejoan, V. Kurdyumov (2019), Thermal expansion effect on the propagation of premixed flames in narrow channels of circular cross-section: Multiplicity of solutions. axisymmetry and non-axisymmetry. *Proc. Combust. Inst.* 37: 1927.
- [9] A. Dejoan, C. Jiménez, V. Kurdyumov (2019), Critical conditions for non-symmetric flame propagation in narrow channels: influence of the flow rate, the thermal expansion, the Lewis number and heat-losses, *Combust. Flame* 209: 430,
- [10] T. Poinso, S. Lele (1992), Boundary conditions for direct simulations of compressible reacting flows, *J. Comp. Physics* 101: 104.
- [11] T. Poinso, D. Veynante, S. Candel (1991), Quenching processes and premixed turbulent combustion diagrams, *J. Fluid Mech.*: 228 (561).
- [12] D. Martínez-Ruiz, F. Veiga-López, D. Fernández-Galisteo, V. Kurdyumov, M. Sánchez Sanz (2019). The role of conductive heat losses on the formation of isolated flame cells in Hele-Shaw chambers *Combust. Flame* 209:187.